

## SUPPORTING INFORMATION

### Mitochondrial Peroxiredoxin Functions as Crucial Chaperone Reservoir in

#### *Leishmania infantum*

Filipa Teixeira<sup>a,b,c,d</sup>, Helena Castro<sup>a,b</sup>, Tânia Cruz<sup>a,b</sup>, Eric Tse<sup>e</sup>, Philipp Koldewey<sup>d</sup>,  
Daniel R. Southworth<sup>e,f</sup>, Ana M. Tomás<sup>a,b,c,1</sup>, Ursula Jakob<sup>d,f,1</sup>

<sup>a</sup>Instituto de Investigação e Inovação em Saúde, Universidade do Porto, 4200 Porto, Portugal

<sup>b</sup>IBMC - Instituto de Biologia Molecular e Celular, Universidade do Porto, 4150-180 Porto, Portugal

<sup>c</sup>ICBAS – Instituto de Ciências Biomédicas Abel Salazar, Universidade do Porto, 4050-313 Porto, Portugal

<sup>d</sup>Department of Molecular, Cellular and Developmental Biology, University of Michigan, Ann Arbor, MI 48109 USA

<sup>e</sup>Life Science Institute, University of Michigan, Ann Arbor, MI 48109, USA

<sup>f</sup>Department of Biological Chemistry, University of Michigan, Ann Arbor, MI 48109 USA

<sup>1</sup>Corresponding authors

Ursula Jakob

Email: [ujakob@umich.edu](mailto:ujakob@umich.edu)

Tel: +1-734-615 1286

Ana M. Tomás

Email: [atomas@ibmc.up.pt](mailto:atomas@ibmc.up.pt)

Tel: +351 226 074 900

**Running Title:** Chaperone Function of mTXNPx is Crucial for Parasite Infectivity

## **Supporting Material and Methods:**

**Chaperone activity assays** - To investigate the chaperone activity of mTXNPx, 100 nM luciferase (Promega), 100 nM citrate synthase (Sigma-Aldrich) or 150 nM malate dehydrogenase (Roche) were incubated in 40 mM HEPES, pH 7.5 at 41.5°C, 43°C or 45°C, respectively, either in the absence or presence of a 20:1 molar ratio of mTXNPx<sub>red</sub> or mTXNPx<sub>ox</sub>. To prepare mTXNPx<sub>red</sub>, mTXNPx<sub>ox</sub> was incubated in the presence of 5 mM DTT or its physiological reducing system consisting of 200 µM NADPH, 0.5 U/ml *L. infantum* trypanothione reductase (TR), 50 µM trypanothione disulfide (TS<sub>2</sub>, Bachem) and 2.5 µM *L. infantum* tryparedoxin 2 (TXN2) for 30 min at 30°C. To test the influence of mTXNPx<sub>red</sub> on chemically denatured client proteins at non-stress temperatures, 12 µM citrate synthase (CS) was incubated for 12 h in 6 M Gnd-HCl or for 4-5 hours in 5 M urea using 40 mM HEPES, pH 7.4 as buffer. Then, CS was diluted to 75 nM (from Gnd-HCl) or 80 nM (from urea) into 40 mM HEPES, pH 7.5 at 30°C in the absence or presence of mTXNPx<sub>red</sub>. Light scattering was measured using a fluorescence spectrophotometer (Hitachi F4500) equipped with a temperature-controlled cuvette holder and stirrer ( $\lambda_{ex/em}$  360 nm, slit widths 2.5 nm).

**Size exclusion chromatography** - To determine the redox dependent oligomerization state of mTXNPx, size-exclusion chromatography (SEC) was performed. Briefly, 125 µg wild-type or mutant mTXNPx<sub>red</sub> or mTXNPx<sub>ox</sub> was applied onto a Superose 12 column, pre-equilibrated with 0.1 M sodium phosphate buffer pH 7.2, 150 mM NaCl. In the case of mTXNPx<sub>red</sub>, the buffer was supplemented with 1 mM DTT to prevent reoxidation of the proteins. Calibration of the column was performed using commercially available molecular mass standards. The concentration of reduced

and oxidized wild-type mTXNPx in the peak area was calculated. Briefly, the average peak concentration of each eluting species on the chromatogram was calculated integrating the area below each peak (at the peak maximum  $\pm$  0.5 ml retention volume) using the Origin software (OriginLab, Northampton, MA). Then the percent area (%p) of each peak compared to the total area of the entire chromatogram was determined, and the average peak concentration ( $c_a$ ) of monomeric mTXNPx was calculated using the following equation:

$$c_a = \frac{\%p * n_t}{M_r * 0.001 \text{ l}}$$

where  $n_t$  is the total amount of loaded mTXNPx (i.e., 125  $\mu$ g) and  $M_r$  depicts the molecular weight of monomeric mTXNPx.

***Isothermal Titration Calorimetry (ITC)*** - ITC experiments of mTXNPx<sub>red</sub> and mTXNPx<sub>ox</sub> were conducted as previously described for other Prx members (1) using an iTC200 (Malvern Instruments Ltd., Malvern, UK). mTXNPx<sub>red</sub> or mTXNPx<sub>ox</sub> were dialysed overnight against 50 mM sodium phosphate buffer, pH 8 supplemented with 1 mM DTT in case of mTXNPx<sub>red</sub>. mTXNPx<sub>red</sub> (50  $\mu$ M) or mTXNPx<sub>ox</sub> (100  $\mu$ M) were loaded into a syringe and titrated into a cell containing the same buffer equilibrated at 25°C. In order to allow the dissociation of mTXNPx to reach equilibrium in the cell, the injection interval was set to 840 sec for the reduced and 600 sec for the oxidized protein, with an initial delay time of 60 sec. The solution was stirred with 1,000 rpm, and the reference power was set to 10  $\mu$ cal s<sup>-1</sup> at high feedback mode. After each experiment, the instrument was washed as recommended by the manufacturer. Data analysis was conducted using a plugin for the software Origin (OriginLab, Northampton, MA) provided by the manufacturer. The heat of dilution from a buffer to

buffer injection was not subtracted from the data since no heat change was observed. The critical transition concentration (CTC) was calculated as described (1, 2). The reaction enthalpy of the decamer dissociation was calculated as the average of the integrated heat pulses (cal per mol mTXNPx monomer) of all injections before reaching the CTC. The first injection was incomplete and therefore disregarded.

**Determination of the intracellular concentration of mTXNPx** - Protein extracts of *L. infantum* stationary phase promastigotes (cultured as described in the main text) and axenic amastigotes (3) were used to estimate the total *in vivo* concentration of mTXNPx. Recombinant purified mTXNPx was used as standard. Proteins were separated using a reducing SDS-PAGE and blotted onto a nitrocellulose membrane. The blot was then incubated with polyclonal anti-mTXNPx rabbit serum (dilution 1:1000). Anti-rabbit IgG conjugated with horseradish peroxidase (dilution 1:10000; Molecular Probes) was used as secondary antibody. The immuno-reaction was detected with Clarity™ western ECL substrate (Biorad) and imaged in a ChemiDoc™ XRS+ imaging system (BioRad). Band intensities were quantified using the Image Lab™ software (BioRad). Concentration of mTXNPx in the different stages of parasite life cycle was estimated based on reported cell volumes (4, 5).

**Negative Staining EM** - mTXNPx<sub>red</sub> (10 μM) alone, luciferase (1 μM) alone, or a mixture of mTXNPx<sub>red</sub> and luciferase were first incubated on ice. Then, the samples were split and incubated for 2 min at room temperature before they were transferred either to 30°C or slowly heated from 30°C to 42°C for 10 min to allow complex formation. All samples were centrifuged at 16,100 xg for 30 min at 4°C to remove potential aggregates. Proteins in the soluble supernatant were then negatively stained using 0.75% (w/v) uranyl formate (pH 5.5-6.0) on 400-mesh carbon-coated copper grids (Pelco) as described in the main text. Samples were imaged under low dose

conditions using a G2 Spirit TEM (FEI) operated at 120 keV. Micrographs were taken at 52,000x magnification with 2.16 Å per pixel using a 4k x 4k CCD camera (Gatan).

### **Supporting Figure Legends:**

#### **Figure S1. Reduced mTXNPx prevents thermal aggregation of different client**

**proteins. A.** Non-reducing SDS-PAGE of purified recombinant mTXNPx in the absence and presence of DTT. **B.** Influence of mTXNPx<sub>ox</sub> upon incubation with its physiologic NADPH/TR/TS<sub>2</sub>/TXN2 reductant-system on the aggregation of luciferase at 41.5°C. A 20:1 molar ratio of mTXNPx to luciferase was used. The control reaction consisted of luciferase incubated with the components of the reducing system in the absence of mTXNPx. The arrow indicates the time point when luciferase was added to the reaction mixture. **C - D.** Influence of DTT-reduced or oxidized mTXNPx (inset) on the thermal aggregation of malate dehydrogenase (MDH) or citrate synthase (CS). Aggregation of MDH and CS was induced at 45°C and 43°C, respectively. A 20:1 molar ratio of mTXNPx to client proteins was used. Control reactions conducted in the absence of mTXNPx<sub>red</sub> were also supplemented with 0.2 mM DTT.

#### **Figure S2. Oligomerization state, $K_D$ and *in vivo* concentration of mTXNPx.**

**A.** The oligomeric states of oxidized (red traces) and reduced (black traces) mTXNPx WT or mTXNPxC81S as determined by size-exclusion chromatography. The concentration of wild-type mTXNPx<sub>red</sub> and mTXNPx<sub>ox</sub> in the elution peak was determined to be 3 µM and 4 µM, respectively. Size exclusion of reduced mTXNPx was conducted in the presence of 1 mM DTT to prevent re-oxidation. The elution volumes of three standard proteins (43, 232 and 440 KDa) are shown. **B.** Determination of the decamer-dimer transition using isothermal titration microcalorimetry (ITC). Representative raw data output (top panel) and integrated

heat pulses (bottom panel) of mTXNPx<sub>red</sub> (left panels) and mTXNPx<sub>ox</sub> (right panels) upon dilution into buffer. In the case of mTXNPx<sub>red</sub>, exothermic heat pulses indicative of a decamer to dimer dissociation were monitored until a critical transition concentration (CTC) of 0.75  $\mu\text{M}$  was reached in the cell. The average reaction enthalpy  $\Delta\text{H}$  of mTXNPx<sub>red</sub> decamer dissociation was determined to be  $644 \pm 61$  cal/mol monomer. In the case of mTXNPx<sub>ox</sub>, no transition was observed indicating that mTXNPx<sub>ox</sub> remains dimeric up to concentrations of at least 100  $\mu\text{M}$ . Averages of CTC as well as reaction enthalpy  $\Delta\text{H}$  were derived from three independent experiments. **C.** Estimation of mTXNPx concentration in *Leishmania infantum* stationary-phase promastigotes and axenic amastigotes. Western blot of increasing quantities of recombinant mTXNPx was used as standard to estimate the concentration of the mTXNPx in stationary-phase promastigotes (P) and axenic amastigotes (A). The respective number of cells used for each experiment is stated below each panel. Protein bands were analyzed by densitometry and protein concentration was calculated using a reported volume of 75 fl and 15 fl for promastigotes and amastigotes, respectively (4, 5). The concentration of mTXNPx for the whole cell was estimated to be 1.6 – 6.1  $\mu\text{M}$  and 49.1 – 102.0  $\mu\text{M}$  for stationary phase promastigotes and amastigotes, respectively. However, since mTXNPx is exclusively mitochondrial, the intracellular concentration reached in mitochondria will be significantly higher. Protein concentration was obtained with two independent experiments. Blots refer to one experiment. Densitometry values that were beyond the values of the standard curve were excluded from the analysis.

**Figure S3. Reduced mTXNPx fails to protect chemically denatured CS at 30°C.**

Influence of mTXNPx<sub>red</sub> on the aggregation of chemically denatured citrate synthase (CS) at 30°C. **A.** GndHCl-denatured CS was diluted into a reaction system containing

a 40:1 molar ratio of reduced or oxidized (inset) mTXNPx to CS. Aggregation of CS was followed by light scattering at 360 nm. The ratio of chaperone to client protein was calculated based on the monomeric form of mTXNPx. Arrow indicates the point at which the client protein was added to the reactions. **B.** Urea-denatured CS was diluted into a reaction system containing a 40:1 molar ratio of mTXNPx<sub>red</sub> to CS. The difference in light scattering signal before and 140 sec after addition of urea-denatured CS was set to 100% aggregation. At least three independent experiments were conducted and the StdDev of three individual measurements is shown.

**Figure S4. Reduced, decameric mTXNPx interacts preferentially with thermally destabilized luciferase.** Negative stain EM of mTXNPx<sub>red</sub> alone or in the presence of luciferase before (i.e., before treatment) or after 10 min incubation at either 30°C or 42°C. Luciferase alone was treated under the same conditions. Samples were centrifuged to remove all aggregated proteins and the supernatant was used for negative stain EM. Representative micrographs and selected single particle projections are shown with scale bars equal to 200 Å for the micrograph images and 50 Å for the boxed particles. This experiment was performed independently of the one shown in Figure 5. The percentage of mTXNPx<sub>red</sub> decamers in complex with luciferase varied between experiments.

**Figure S5. Generation of *L. infantum* transfectants expressing an N-terminally tagged mTXNPx mutant variant.** **A.** Map of the *pSSU-PHLEO-infantum-MTS.His.THR-mTXNPx* construct used for complementation of previously generated *mtxnp<sup>x</sup>-L. infantum* parasites (6). The *His.THR-mTXNPx* fragment was PCR-amplified from pET28c-His.THR-mTXNPx with primers P1 and P2 (Table S1), and cloned into the SacII/XbaI sites of *pSSU-PHLEO-infantum-mTXNPx*. The resulting construct was linearized by digestion with NdeI+PmeI prior to electroporation of

*mtxnp<sup>x-</sup>* promastigotes. Depicted in the scheme are the restriction sites (NdeI, SacII, XbaI and PmeI) relevant for molecular biology procedures. The endogenous mitochondrial targeting sequence (MTS) and the *mTXNPx* ORF encoding the mature protein are shown in orange, and the histidine-thrombin (His.THR) in red. Also illustrated is the amino acid sequence of His.THR. Grey boxes represent the 5' and 3' coding regions of the small subunit 18S rRNA (SSU) of *L. infantum*, required for integration of the construct into the SSU locus by homologous recombination. Grey-framed white boxes refer to the splice leader acceptor site (SAS), as well as to the cysteine proteinase B intergenic region (CPB IR) cloned downstream of *MTS.His.THR-mTXNPx* and of *PHLEO* to guarantee adequate expression of both genes. **B.** Genomic organization of the small subunit 18S rRNA (SSU) locus of *mtxnp<sup>x-</sup>/+MTS.His.THR-mTXNPx* mutants with the integrated *PHLEO* construct (represented by the thick line). Arrowheads show the location of primers used for PCR diagnosis of the transfectants (in C.). **C.** PCR analysis of genomic DNA from *mtxnp<sup>x-</sup>*, *mtxnp<sup>x-</sup>/+mTXNPx*, and two independent *mtxnp<sup>x-</sup>/+MTS.His.THR-mTXNPx* promastigote clones, using specific primers to amplify the *mTXNPx* ORF (P7/P2), to diagnose for the presence of the *PHLEO* cassette (P7/P8) and its correct integration into the ribosomal locus (P9/P10), and to detect the *MTS.His.THR-mTXNPx* chimera (P1/P2) (primer location is represented in A.).

## **References**

1. Barranco-Medina S & Dietz KJ (2009) Thermodynamics of 2-Cys peroxiredoxin assembly determined by isothermal titration calorimetry. *Methods Enzymol* 466:409-430.
2. Barranco-Medina S, Kakorin S, Lazaro JJ, & Dietz KJ (2008) Thermodynamics of the dimer-decamer transition of reduced human and plant 2-cys peroxiredoxin. *Biochemistry* 47(27):7196-7204.

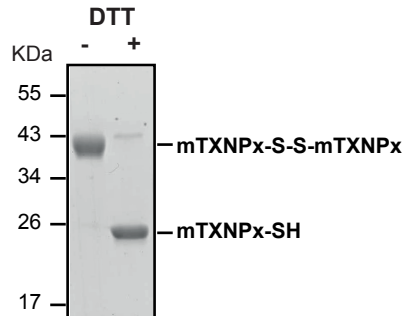
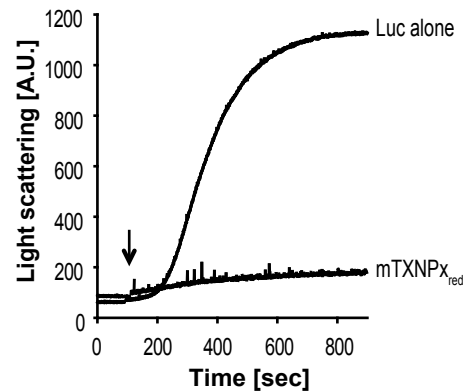
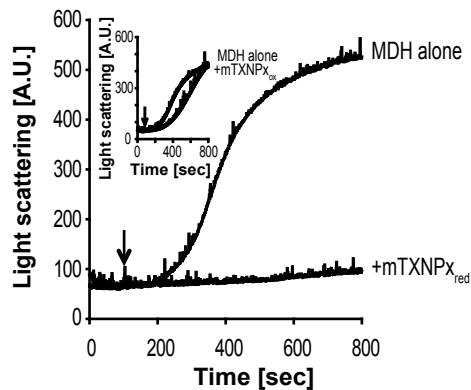
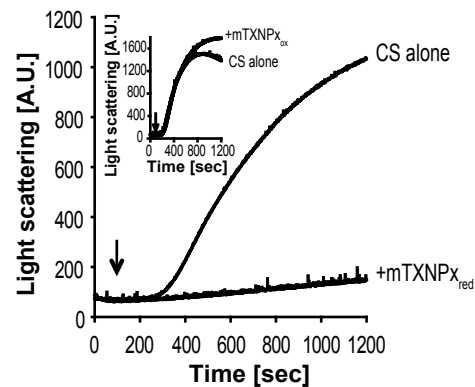


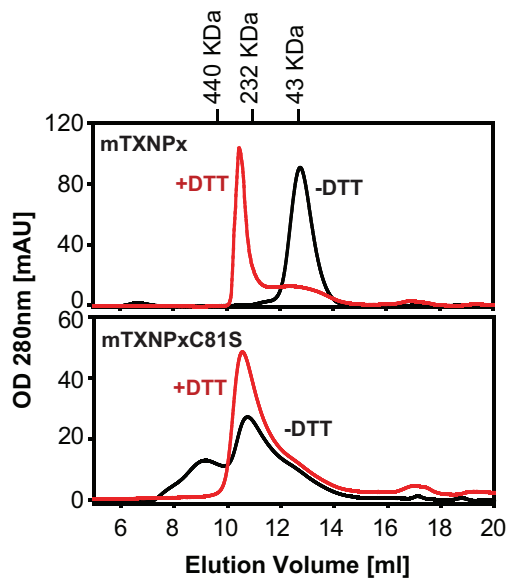
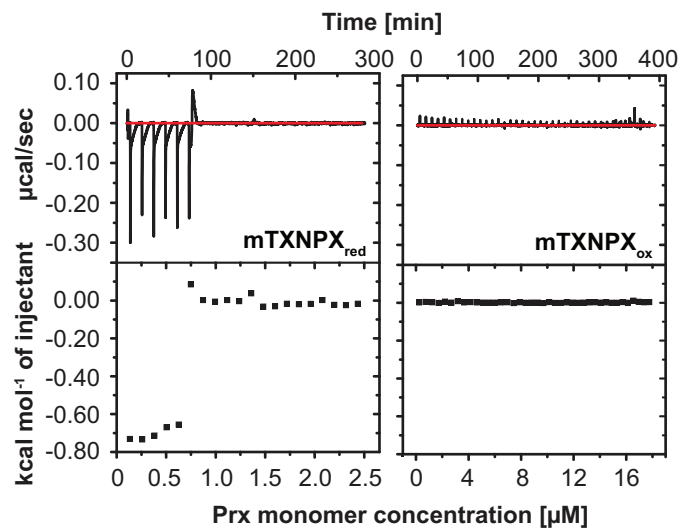
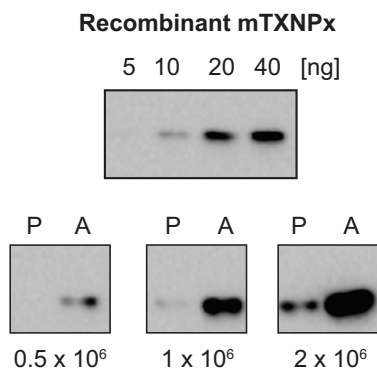
3. Sereno D, *et al.* (1998) Axenically grown amastigotes of *Leishmania infantum* used as an in vitro model to investigate the pentavalent antimony mode of action. *Antimicrobial agents and chemotherapy* 42(12):3097-3102.
4. Sousa Silva M, Ferreira AE, Tomas AM, Cordeiro C, & Ponces Freire A (2005) Quantitative assessment of the glyoxalase pathway in *Leishmania infantum* as a therapeutic target by modelling and computer simulation. *The FEBS journal* 272(10):2388-2398.
5. Romao S, Castro H, Sousa C, Carvalho S, & Tomas AM (2009) The cytosolic trypanothione of *Leishmania infantum* is essential for parasite survival. *Int J Parasitol* 39(6):703-711.
6. Castro H, *et al.* (2011) *Leishmania* mitochondrial peroxiredoxin plays a crucial peroxidase-unrelated role during infection: insight into its novel chaperone activity. *PLoS Pathog* 7(10):e1002325.

**Table S1. List of oligonucleotides used in this work.**

Primer number	Primer sequence
P1	5'GCAGTT <b>CCGCGGG</b> TTTCGCGGCTACGTCGCCGCTTTTGATGGGCAGCAGCCATCATCATC-3'
P2	5'-tgc <i>tctaga</i> TCACATGTTCTTCTCGAAAAAC-3'
P3	5'-CTGGTGCCAGCACCA <u>G</u> CGGTAATTCCAGC-3'
P4	5'-GCTGGAATTACCGC <u>I</u> GGTGCTGGCACCAG-3'
P5	5'-CCGCGCGGCAGCCA <u>C</u> ATGAATCTGGACTA-3'
P6	5'-TAGTCCAGATTCAT <u>G</u> TGGCTGCCGCGCGG-3'
P7	5'-cgc <i>ggatcc</i> ATGCTCCGCCGTCTTCCCA-3'
P8	5'-CCACTGCCGCAGCGTT-3'
P9	5'-GCGGTGTGTACAAATGGC-3'
P10	5'-gg <i>actagf</i> TCAGTCCTGCTCCTCGGC-3'

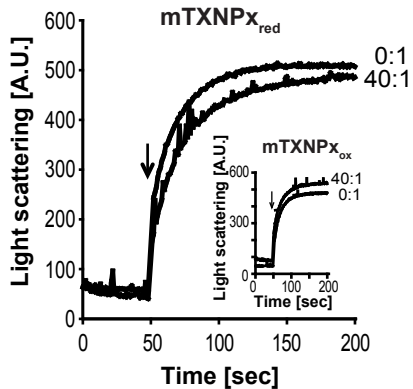
Clamp sequences are indicated in lower case, restriction sites in bold/italic, and mutations introduced by site directed mutagenesis underlined.

**Figure S1****A****B****C****D**

**Figure S2****A****B****C**

**Figure S3**

**A**



**B**

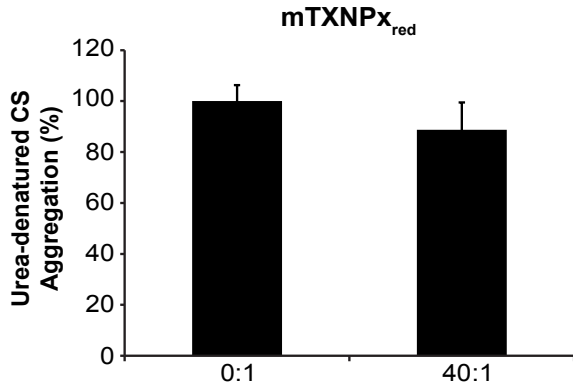


**Figure S4**

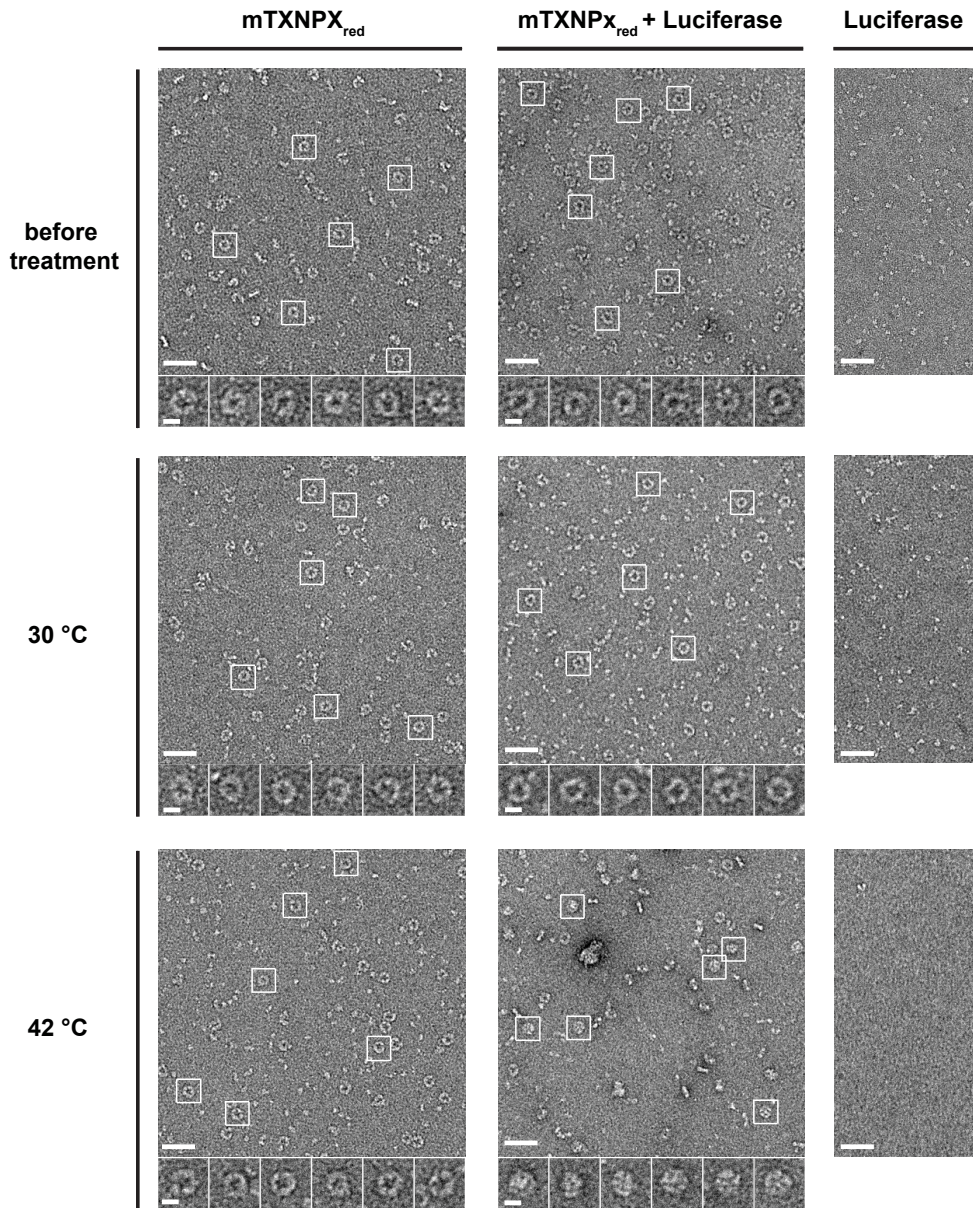
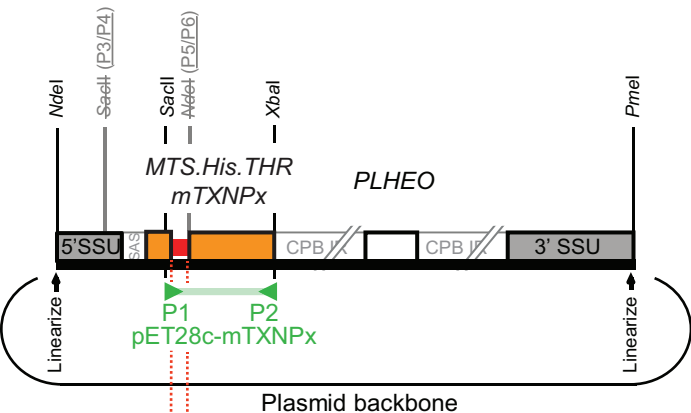


Figure S5

A

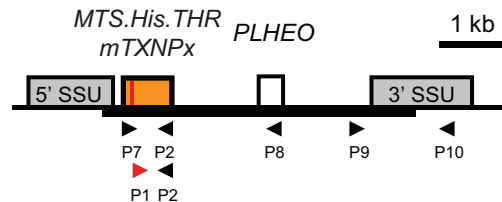


MGSSHHHHHHSSSGLVPRGSHM

His-tag

Thrombin  
cleavage site

B



C

